INSTITUTE OF PHYSICS PUBLISHING JOURNAL OF PHYSICS B: ATOMIC, MOLECULAR AND OPTICAL PHYSICS

J. Phys. B: At. Mol. Opt. Phys. **39** (2006) 3447–3455 doi:10.1088/0953-4075/39/17/003

Observation of the widening and shifting of EIT windows in a quasi-degenerate two-level atomic system

Yabin Dong, Junxiang Zhang, Haihong Wang and Jiangrui Gao

State Key Laboratory of Quantum Optics and Quantum Optics Devices, Institute of Opto-Electronics, Shanxi University, Taiyuan 030006, People's Republic of China

E-mail: zhangjxparis@yahoo.com

Received 22 July 2005, in final form 10 January 2006
Published 14 August 2006
Online at stacks.iop.org/JPhysB/39/3447

Abstract

Widening and shifting the EIT windows in a closed transition $F_e = 2 \leftrightarrow F_g = 3$ driven by linearly polarized coupling lights and probed by circularly polarized lights are observed in Cs vapour. It is shown that by increasing the strength of magnetic field i.e. Zeeman splitting in the upper and lower levels, the electromagnetically induced transparency window is divided into two windows and the EIT maxima are shifted away from the zero detuning. In the contrast, if the strength of the magnetic field is fixed and the Rabi frequency of coupling beam is increased, the two EIT windows become wider, and the gap between the two EIT windows becomes smaller and smaller. These effects are also theoretically discussed and they are qualitatively in agreement with the theoretical results.

(Some figures in this article are in colour only in the electronic version)

1. Introduction

It is well known that quantum coherence and interference between atomic states can lead to many interesting and important phenomena, such as electromagnetically induced transparency (EIT) [1], electromagnetically induced absorption (EIA) [2], coherent population trapping (CPT) [3], lasing without inversion (LWI) [4] etc. In addition, they have many applications in the enhancement of the refractive index [5], slow light and storage of quantum information in a coherent medium [6], the design of highly sensitive magnetometers [7], quantum computation [5], the quantum logic gate [8], quantum switches [9] and quantum interferometric optical lithography [10].

In the past, most of the investigations about quantum coherence were carried out in three-level atomic systems, in which an atomic coherence of EIT was induced in an atomic system by two distinct optical fields (coupling and probe fields). However in a practical atomic system, atomic transitions often involve magnetic sublevel structures that can lead to interesting

and complex variations of absorption due to the coherence between the coupling field and the Zeeman splitting. Recently Akulshin and co-workers reported the first experimental observation of EIA in a degenerate two-level atomic system [2]. Later, they analysed the spontaneous transfer of the atomic coherence (TOC) between degenerate excited states to the atomic coherence between degenerate ground states that played a key role in the occurrence of EIA (called EIA-TOC) [11, 12], and discussed the dependence of EIA on the field polarization [13]. Goren *et al* [14] concluded that not only the TOC but also the collision transfer of population (TOP) from the ground state to a reservoir can lead to EIA peaks in the absorption spectrum of a degenerate two-level system, and explained why EIA can also occur in open systems, and also why it occurs when the coupling and probe beams interacting with a closed $F_g \leftrightarrow F_e = F_g + 1$ with $F_g > 0$ hyperfine transition have the same polarization rather than different polarization as in the case of the EIA-TOC. Furthermore, it was reported that the EIA effect in an open system regardless of angular momentum was experimentally obtained in a degenerate two-level atomic system [15]. Ying Gu *et al* theoretically studied the quantum coherence effects induced by the competition between the coupling field and the Zeeman splitting in a degenerate two-level atomic ensemble; it is predicted that the possible transition from EIT to EIA due to the shifting and widening of EIT windows can happen for closed transitions $F_e = 0 \leftrightarrow F_g = 1$ and $F_e = 1 \leftrightarrow F_g = 2$ when the atomic system is driven by linearly polarized π light and probed by transverse light with two equal left and right components $\sigma_\pm$ [16, 17]. The experimental demonstration of Gaussian light pulse propagation from subluminal to superluminal based on the transition from EIT to EIA by changing only the power of coupling light was done in the Cs D2 line of $6^2S_{1/2}(F_g = 4) \leftrightarrow 6^2P_{3/2}(F_e = 5)$ [18].

In comparison with the typical three-level system, the degenerate two-level system (DTLS) can give rise to a wealth of different configuration coupled by the optical fields [19]. In DTLS, the actual number of involved sublevels is larger and this introduces diversity in the matrix elements describing the atom–field coupling, thus the system could be treated as the superposition of several three-level and pure two-level subsystems; the absorption spectrum is a combination of EIT and Mollow absorption spectra. Because of the competition between the EIT and absorption effects due to the interplay between the dominance of Rabi frequency and Zeeman splitting, the multi-coherence will be involved in DTLS. In this work, we experimentally discuss the effects of competition between the Rabi frequency of the coupling beam and the Zeeman splitting on EIT in the transition $F_e = 2 \leftrightarrow F_g = 3$ of D2 line of a Cs ensemble. The splitting, widening and shifting of EIT windows are observed. And furthermore, we qualitatively compare these experimental results with numerical calculations. The splitting of EIT window due to the Zeeman splitting was always reported in a three-level atomic system [20]. It was shown that a single EIT window became wider and its transparency maximum was shifted when a detuned coupling beam was applied in the three-level atomic system [21]. In this study, a degenerate two-level atomic system is involved in discussion about the multilevel induced coherence. Because of the Zeeman splitting, a single EIT window is divided into two symmetrical EIT windows, and both of the two transparency maxima become wider and shift their position with the increase in the power of the coupling beam and the magnetic field. This effect might be developed in subluminal and controllable propagation of more than one slow pulse lights in an atomic system.

2. Experimental set-up and results

The hyperfine energy levels structure of the caesium atom is shown in figure 1. The transition $6S_{1/2}(F_g = 3) \leftrightarrow 6P_{3/2}(F_e = 2)$ of the Cs D_2 line is employed as a degenerate

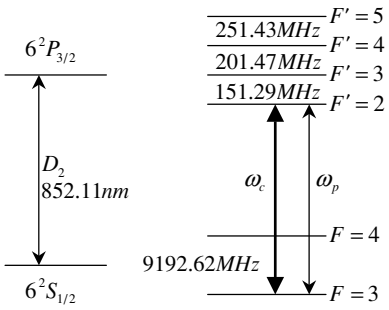

Figure 1. The energy level configuration of Cs D_2 line.

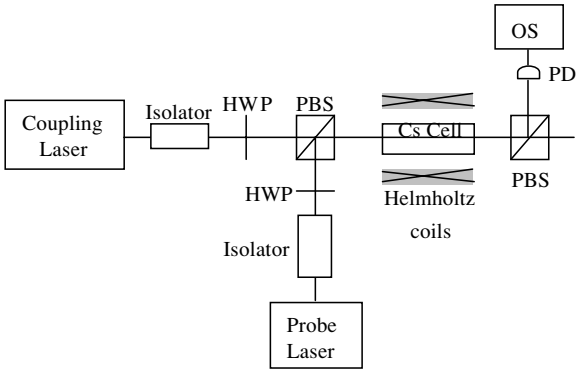

Figure 2. The experimental set-up. PBS: polarizing beam splitter; PD: photodetector; HWP: half-wave plate; OS: oscilloscope.

two-level system, the coupling and probe laser lights with frequency of ω_c and ω_p are interacted with the two-level system, and they propagate in the same direction (i.e. Doppler-free configuration) through the Cs atoms cell. Due to the Doppler-free configuration, the same groups of atoms 'see' both the coupling and probe beams on resonance with transition $6S_{1/2}(F_g = 3) \leftrightarrow 6P_{3/2}(F_e = 2)$ at the same time. In this case, the system is considered as a closed system since there is no more possibility for atoms in excited state decay to the ground level $6S_{1/2}(F_g = 4)$ because of selection rules for electric dipole transition.

The experimental set-up is shown in figure 2. Two external cavity diode lasers (TOPTICA; DL100) with less than 1 MHz line width are used as coupling and probe laser lights, respectively. Both of the two beams have been spatially filtered to produce a quasi-Gaussian beam profile with a beam diameter of 2 mm. The coupling laser is locked to the resonant frequency of $6S_{1/2}(F_g = 3) \leftrightarrow 6P_{3/2}(F_e = 2)$ transition; it propagates through the optical isolator and half-wave plate, and then passes through a 5 cm long Cs cell at room temperature. The probe light is scanned by a piezoelectric ceramic in the vicinity of the transition $6S_{1/2}(F_g = 3) \leftrightarrow 6P_{3/2}(F_e = 2)$, the beam passes through the other isolator and half-wave plate, and overlaps with the coupling laser by a polarizing beam splitter before the Cs cell. The extinction ratios of the polarizing beam splitter are greater than 25 dB, thus the polarizations of two beams are well linearly polarized and their polarizations are orthogonal to each other. The frequencies of two lasers are monitored using Doppler-free saturated absorption spectroscopy. In order to define the coupling beam as the π polarization,

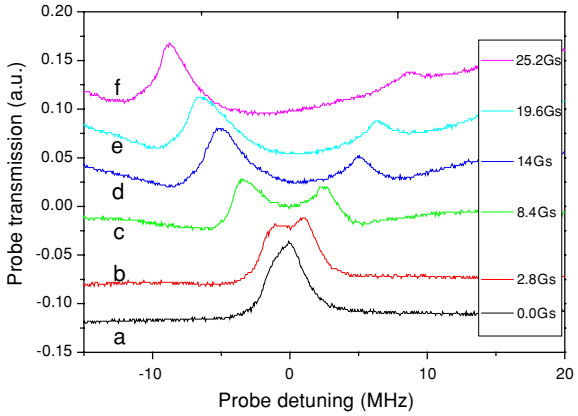

Figure 3. The transmission spectra of the probe beam as a function of probe detuning with different magnetic field strengths B. The intensity of the coupling and probe lights are $P_c = 3.36$ mW and $P_p = 0.304$ mW. (a) EIT spectrum with the strengths of magnetic field $B = 0$ Gs. ((b)–(f)) Separated and shifted EIT peaks with $B = 2.8$ Gs in curve b; $B = 8.4$ Gs in curve c; $B = 14$ Gs in curve d; $B = 19.6$ Gs in curve e; $B = 25.2$ Gs in curve f.

we apply a weak magnetic field along the polarization direction of the coupling beam by a pair of Helmholtz coils, the quantization axis of magnetic field is perpendicular to the polarization direction of the probe light; we can treat the probe light as a transverse light with two equal left and right components $\sigma_{\pm}$. After passing through the Cs cell, a polarizing beam splitter separates the probe and coupling beams, and only the probe beam is detected by photodiode and recorded by a digital oscilloscope.

Figure 3 shows the transmission spectra of a probe beam as a function of the probe detuning with different strength of magnetic field B. The total Rabi frequencies of the coupling and probe lights are fixed to be $Z_c = 29.6$ MHz and $Z_p = 8.9$ MHz respectively, which is deduced from the definition about the Rabi frequency of light $\Omega = \Gamma \times \sqrt{\frac{I}{2I_0}}$, here $I = \frac{P}{\pi r^2}$ mW cm^{-2} is the power density of the field, and the saturation intensity is $I_0 = 1.65$ mW cm^{-2}. The corresponding powers of coupling and the probe beams are 3.36 mW and 304 μW. The strength of the Helmholtz coils is tuned from 0 Gs up to 25.2 Gs, as shown in figures 3(a)–(f).

During the measurement process, the frequency of a coupling laser is locked to the line of $F = 3(6S_{1/2}) \leftrightarrow F' = 2(6P_{3/2})$ using a standard technology of a saturation absorption spectrum; the probe laser is scanned across the transition of $F = 3(6S_{1/2}) \leftrightarrow F' = 2(6P_{3/2})$. When we switch off the magnetic field, as is expected for quantum coherence in general degenerate two-level system, the transmission of probe laser after the vapour cell shows that the EIT effect is observed, as is shown in figure 3(a). If we switch on the magnetic field, the degeneracy of both excited and ground levels is broken, and the Zeeman sublevels appear. Because of the coherence between the Zeeman sublevels and coupling field, and also the coherence among the Zeeman sublevels, the transmission spectra change. It is seen in figure 3(b) that the transparency peak begins to split. When the strength of magnetic field B is continuously increased, the EIT window breaks up into two peaks with a gap between them as shown in figure 3(c). Furthermore when the strength of magnetic field B is increased to be larger, the two peaks get apart from each other as seen in figures 3(d)–(f). And it is obviously seen that both the two transparency maxima shift their position away from the region of zero detuning with the strength of magnetic field increasing.

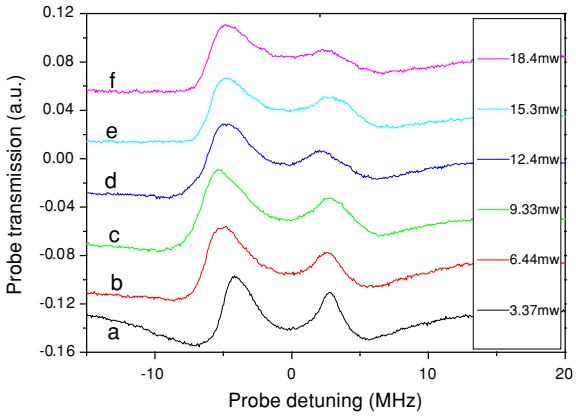

Figure 4. The transmission spectra depending on the intensity of the coupling beam. The strengths of magnetic field and probe beam are $B = 9.8$ Gs and $P_p = 0.304$ mW. ((a)–(f)) The two EIT peaks become wider with the intensity of the coupling beam increasing. Curve a for $P_c = 3.37$ mW; curve b for $P_c = 6.44$ mW; curve c for $P_c = 9.33$ mW; curve d for $P_c = 12.4$ mW; curve e for $P_c = 15.3$ mW; curve f for $P_c = 18.4$ mW.

Figure 4 shows the transmission spectra with varying the intensity of coupling beam when the strengths of magnetic field B and probe beam are fixed. The strengths of magnetic field B and the power of probe beam are taken to be 9.8 Gs and 304 μW, respectively. It is seen in figures 4(a)–(f) that both the two EIT windows become wider as the intensity of coupling beam is increased from 3.37 mW to 18.4 mW, which correspond to the Rabi frequency from 29.6 MHz to 69.5 MHz. It causes the effect that the gap between two EIT windows becomes smaller and smaller.

It may be noted that the separated two EIT windows should be symmetrical in their heights and positions. The experimental results we obtained show that the two windows are not in a good symmetrical pattern as we predict. It mainly comes from the effect of Doppler broadening, which is theoretically discussed in the following part.

In order to find a qualitative explanation of above phenomena, we use the theoretical model proposed by Ying Gu *et al* [17] for transition $F_g = 2 \leftrightarrow F_e = 1$ to get the numerical calculation for the transition $F_g = 3 \leftrightarrow F_e = 2$, which satisfy the conditions $F_g > F_e$ and $F_g, F_e < 0$.

3. The theoretical analysis

Figure 5 shows a degenerate two-level system for transition $F_g = 3 \leftrightarrow F_e = 2$. It is driven by a linearly polarized σ field with frequency ω_c and probed by circularly polarized $\sigma_\pm$ field with frequency ω_p. The excited states are expressed as $|e_{-2}\rangle$, $|e_{-1}\rangle$, $|e_0\rangle$, $|e_1\rangle$ and $|e_2\rangle$, while the ground states are $|g_{-3}\rangle$, $|g_{-2}\rangle$, $|g_{-1}\rangle$, $|g_0\rangle$, $|g_1\rangle$, $|g_2\rangle$ and $|g_3\rangle$. The system is assumed to be closed without leakage to the outside. Only the decay of the atomic levels Γ due to the spontaneous emission, as well as the decay Γ_0 between the ground sublevel states or excited sublevel states resulted from collisions is considered. In rotating-wave approximation, the evolution equations for the atomic variables are given by

$$\dot{\rho}_{e_i g_j} = \frac{i}{\hbar}\left[\sum_k \left(V_{e_i g_k}\rho_{g_k g_j} - \rho_{e_i e_k}V_{e_k g_j}\right)\right] - \left(i\omega_{e_i g_j} + \gamma_{eg}\right)\rho_{e_i g_j}, \tag{1}$$

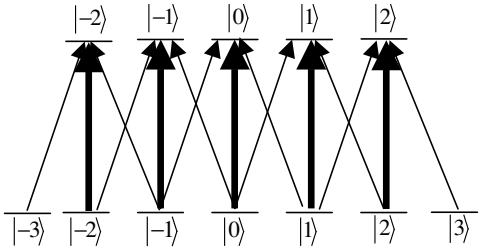

Figure 5. Schematic energy level diagrams for transition $F_e = 2 \leftrightarrow F_g = 3$ driven by linearly polarized π light and probed by circularly polarized $\sigma_\pm$ light.

$$\dot{\rho}_{e_i e_i} = \frac{i}{\hbar}\sum_k \left(V_{e_i g_k}\rho_{g_k e_i} - \rho_{e_i g_k}V_{g_k e_i}\right) - \left(7\Gamma + 4\Gamma_0\right)\rho_{e_i e_i} + \Gamma_0 \sum_{j\neq i}\rho_{e_j e_j}, \tag{2}$$

$$\dot{\rho}_{e_i e_j} = \frac{i}{\hbar}\sum_k \left(V_{e_i g_k}\rho_{g_k e_j} - \rho_{e_i g_k}V_{g_k e_j}\right) - \left(i\omega_{e_i e_j} + \gamma_{ee}\right)\rho_{e_i e_j}, \tag{3}$$

$$\dot{\rho}_{g_i g_i} = \frac{i}{\hbar}\sum_k \left(V_{g_i e_k}\rho_{e_k g_i} - \rho_{g_i e_k}V_{e_k g_i}\right) - 6\Gamma_0\rho_{g_i g_i} + \Gamma\sum_{i=-2}^{2}\rho_{e_i e_i} + \Gamma_0\sum_{j\neq i}\rho_{g_j g_j}, \tag{4}$$

$$\dot{\rho}_{g_i g_j} = \frac{i}{\hbar}\sum_k \left(V_{g_i e_k}\rho_{e_k g_j} - \rho_{g_i e_k}V_{e_k g_j}\right) - \left(i\omega_{g_i g_j} + \gamma_{gg}\right)\rho_{g_i g_j}, \tag{5}$$

where $\omega_{e_i e_j} = \omega_{e_i} - \omega_{e_j}$ and $\omega_{g_i g_j} = \omega_{g_i} - \omega_{g_j}$ denote the Zeeman splitting of excited state and ground states, respectively; $\omega_{k_i k_j} = g_k\mu_b B/\hbar$ $(i = j \pm 1)$ is the Raman detuning induced by the magnetic field B, where g_k is the Lande factor for $k = e$ or g, and μ_b is the Bohr magnetron; $\omega_{e_i g_j} = \omega_{e_i} - \omega_{g_j}$ is the transition frequency between excited and ground degenerate levels. The $\gamma_{ee} = 7\Gamma + 4\Gamma_0$ is the decay rate of the excited-state coherence, modelling collisions. $\gamma_{gg} = 6\Gamma_0$ is the decay rate of the ground-state coherence, modelling collisions. $\gamma_{eg} = \frac{1}{2}(7\Gamma + 10\Gamma_0)$ is the transition decay rate between the excited states and ground states. Ignoring the effect of spatial amplitude, the interaction energies for the transition $|e_i\rangle \leftrightarrow |g_j\rangle$ are written as $V_{e_i g_j} = \hbar V_{e_i g_j}(\omega_p)\, e^{-i\omega_p t}$ and $V_{e_i g_i} = \hbar V_{e_i g_i}(\omega_c)\, e^{-i\omega_c t}$ with $i = 0, \pm1, \pm2$, $j = i \pm 1$. Here the magnitudes of $2V_{e_i g_j}(\omega_p) = \mu_{e_i g_j}E_p/2^{1/2}\hbar$ and $2V_{e_i g_i}(\omega_c) = \mu_{e_i g_i}E_c/2^{1/2}\hbar$ are defined as the probe and the drive Rabi frequency, respectively. Let $V_{e_i g_j}(\omega_p)$ and $V_{e_i g_j}(\omega_c)$ be real for simplicity. The dipole moments of transitions are

$$\mu_{e_{-1}g_{-2}} = \mu_{e_1 g_2} = -\sqrt{\tfrac{5}{21}}\mu, \qquad \mu_{e_{-1}g_0} = \mu_{e_1 g_0} = -\sqrt{\tfrac{1}{7}}\mu, \qquad \mu_{e_0 g_{-1}} = \mu_{e_0 g_1} = -\sqrt{\tfrac{1}{14}}\mu,$$
$$\mu_{e_{-1}g_{-1}} = \mu_{e_1 g_1} = -\sqrt{\tfrac{4}{21}}\mu \qquad \text{and} \qquad \mu_{e_0 g_0} = -\sqrt{\tfrac{3}{14}}\mu$$

for a Cs atom [22].

Considering the condition that the coupling light is much stronger than probe light, we treat coupling field to all orders in its Rabi frequency and meanwhile probe field to first order, then $\rho_{e_i g_j}$ oscillates at three frequencies [23, 24]: the pump frequency ω_c, the probe frequency ω_p and the four-wave mixing frequency $2\omega_c - \omega_p$. We therefore express $\rho_{e_i g_j}$ in terms of its Fourier amplitudes as

$$\rho_{e_i g_j} = \rho_{e_i g_j}(\omega_p)\, e^{-i\omega_p t} + \rho_{e_i g_j}(2\omega_c - \omega_p)\, e^{-i(2\omega_c - \omega_p)t}, \tag{6}$$

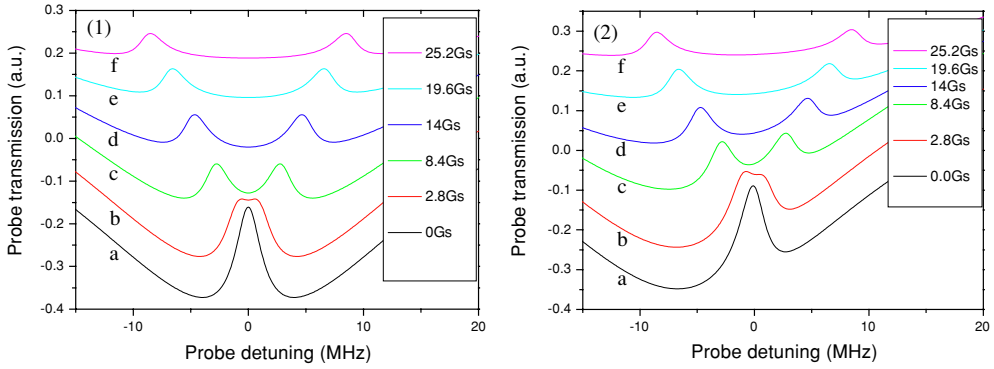

Figure 6. The theoretical transmission spectra of the probe beam versus probe detuning with different strengths of magnetic field B. (1) $k_{\mathrm{p,c}}v = 0$; (2) $k_{\mathrm{p,c}}v = \Gamma$. The intensities of the coupling and probe lights are $V_{\mathrm{c}} = 5.92$ MHz and $V_{\mathrm{p}} = 0.89$ MHz. Curves a, b, c, d, e and f are for $B = 0$ Gs, $B = 2.8$ Gs, $B = 8.4$ Gs, $B = 14$ Gs, $B = 19.6$ Gs and $B = 25.2$ Gs.

and $\rho_{\mathrm{e}_i\mathrm{g}_i}$ in terms of its Fourier amplitudes as

$$\rho_{\mathrm{e}_i\mathrm{g}_i} = \rho_{\mathrm{e}_i\mathrm{g}_i}(\omega_{\mathrm{c}})\,\mathrm{e}^{-\mathrm{i}\omega_{\mathrm{c}}t} + \rho_{\mathrm{e}_i\mathrm{g}_i}(2\omega_{\mathrm{c}} - \omega_{\mathrm{p}})\,\mathrm{e}^{-\mathrm{i}(2\omega_{\mathrm{c}}-\omega_{\mathrm{p}})t}. \tag{7}$$

Similarly, the populations and coherences within the same hyperfine level can be written as

$$\rho_{k_ik_j} = \rho^{dc}_{k_ik_j} + \rho_{k_ik_j}(\omega_{\mathrm{c}} - \omega_{\mathrm{p}})\,\mathrm{e}^{-\mathrm{i}(\omega_{\mathrm{c}}-\omega_{\mathrm{p}})t} + \rho_{k_ik_j}(\omega_{\mathrm{p}} - \omega_{\mathrm{c}})\,\mathrm{e}^{-\mathrm{i}(\omega_{\mathrm{p}}-\omega_{\mathrm{c}})t}, \tag{8}$$

where $\rho_{k_ik_j}(\omega_{\mathrm{c}} - \omega_{\mathrm{p}})\,\mathrm{e}^{-\mathrm{i}(\omega_{\mathrm{c}}-\omega_{\mathrm{p}})t}$ and $\rho_{k_ik_j}(\omega_{\mathrm{p}} - \omega_{\mathrm{c}})\,\mathrm{e}^{-\mathrm{i}(\omega_{\mathrm{p}}-\omega_{\mathrm{c}})t}$ are population and coherence oscillations at frequencies $\omega_{\mathrm{c}} - \omega_{\mathrm{p}}$ and $\omega_{\mathrm{p}} - \omega_{\mathrm{c}}$, respectively. The system is closed, so it satisfies the relation: $\sum_i \rho_{\mathrm{e}_i\mathrm{e}_i} + \sum_j \rho_{\mathrm{g}_j\mathrm{g}_j} = 1$ with $i = 0,\ \pm1, \pm2,\ j = 0,\ \pm1, \pm2, \pm3$. Initially, the atoms have equal incoherent population in the ground-state sublevels.

The probe absorption is calculated from the imaginary part of the susceptibility $\chi(\omega_{\mathrm{p}})$. For transition $F_{\mathrm{e}} = 2 \leftrightarrow F_{\mathrm{g}} = 3$, we have

$$\begin{aligned}\mathrm{Im}\chi(\omega_{\mathrm{p}}) \propto \mathrm{Im}\Big\{\Big[&\mu_{\mathrm{e}_{-2}\mathrm{g}_{-3}}\big(\rho_{\mathrm{e}_{-2}\mathrm{g}_{-3}}(\omega_{\mathrm{p}}) + \rho_{\mathrm{e}_2\mathrm{g}_3}(\omega_{\mathrm{p}})\big) + \mu_{\mathrm{e}_{-2}\mathrm{g}_{-1}}\big(\rho_{\mathrm{e}_{-2}\mathrm{g}_{-1}}(\omega_{\mathrm{p}}) + \rho_{\mathrm{e}_2\mathrm{g}_1}(\omega_{\mathrm{p}})\big)\\ &+ \mu_{\mathrm{e}_{-1}\mathrm{g}_{-2}}\big(\rho_{\mathrm{e}_{-1}\mathrm{g}_{-2}}(\omega_{\mathrm{p}}) + \rho_{\mathrm{e}_1\mathrm{g}_2}(\omega_{\mathrm{p}})\big) + \mu_{\mathrm{e}_{-1}\mathrm{g}_0}\big(\rho_{\mathrm{e}_{-1}\mathrm{g}_0}(\omega_{\mathrm{p}})\rho_{\mathrm{e}_1\mathrm{g}_0}(\omega_{\mathrm{p}})\big)\\ &+ \mu_{\mathrm{e}_0\mathrm{g}_{-1}}\big(\rho_{\mathrm{e}_0\mathrm{g}_{-1}}(\omega_{\mathrm{p}}) + \rho_{\mathrm{e}_0\mathrm{g}_1}(\omega_{\mathrm{p}})\big)\Big]\Big/\big(V_{e_0g_{-1}}/\gamma_{eg}\big)\Big\}.\end{aligned} \tag{9}$$

To model the quantum coherence effects of the $F_{\mathrm{e}} = 2 \leftrightarrow F_{\mathrm{g}} = 3$ transition shown in figure 5, we first define the parameters in Bloch equations. We set $\Gamma = 5.2$ MHz, i.e. the natural line width of Cs D_2 line [22, 25]. So it can be deduced that $\gamma_{\mathrm{eg}} = \frac{7\Gamma+10\Gamma_0}{2} = 19.0$ MHz, $\Gamma_0 = 0.03\Gamma = 0.156$ MHz, $\gamma_{\mathrm{ee}} = 7\Gamma + 4\Gamma_0 = 37.0$ MHz and $\gamma_{\mathrm{gg}} = 6\Gamma_0 = 0.936$ MHz. The drive field detuning is $\Delta = \omega_{\mathrm{c}} - \omega_{\mathrm{e}_0\mathrm{g}_0}$, and the probe field detuning is $\delta = \omega_{\mathrm{p}} - \omega_{\mathrm{e}_0\mathrm{g}_0}$.

When a magnetic field is present, the Zeeman splitting in the excited and ground states occurs simultaneously, the degeneracy of the two-level system is broken. In this case, not only the coherence between the Zeeman splitting and coupling field, but also the coherence among the Zeeman sublevels, should be considered. Note that the Zeeman splitting $\Delta e (or\, \omega_{\mathrm{e}_1\mathrm{e}_0})$ of the excited state is always not equal to the splitting $\Delta g\big(or\ \omega_{\mathrm{g}_1\mathrm{g}_0}\big)$ of the ground state. According to the data of Cs atoms for the hyperfine levels of $6S_{1/2}$, $F_{\mathrm{g}} = 3$ and $6P_{3/2}$, $F_{\mathrm{e}} = 2$, we take $\Delta e = \mu_{\mathrm{B}} \times g_{\mathrm{F}} \times B/\hbar$ ($g_{\mathrm{F}} = 2/3$), $\Delta g = \mu_{\mathrm{B}} \times g'_{\mathrm{F}} \times B/\hbar$ ($g'_{\mathrm{F}} = 1/4$).

The theoretical transmission spectra of the probe beam as a function of the probe detuning for different strengths of magnetic field B are shown in figure 6(1). The intensity of the coupling and probe lights are taken to be $V_{\mathrm{c}} = V_{\mathrm{e}_i\mathrm{g}_i}(\omega_{\mathrm{c}}) = 5.92$ MHz ($i = 0,\ \pm1$),

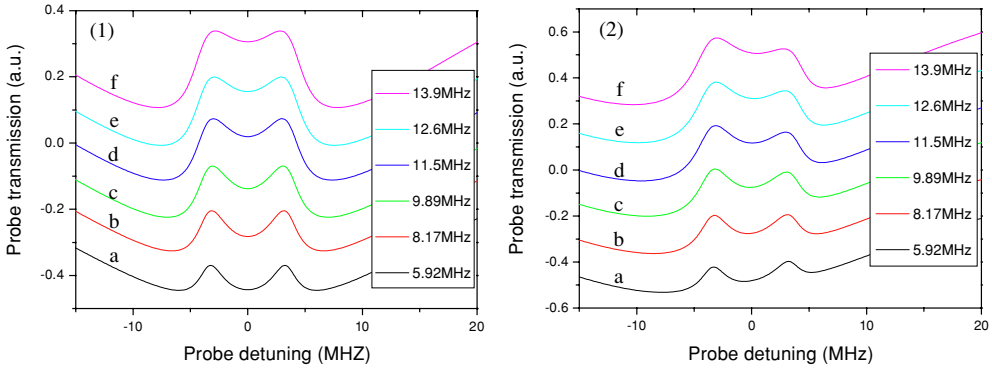

Figure 7. The theoretical transmission spectra of the probe beam depending on the intensity V_c of the coupling beam with fixed strength of magnetic field $B = 9.8$ Gs and probe beam $V_p = 0.89$ MHz. (1) $k_{p,c}v = 0$; (2) $k_{p,c}v = \Gamma$. $V_c = 5.92$ MHz in curve a; $V_c = 8.17$ MHz in curve b; $V_c = 9.89$ MHz in curve c; $V_c = 11.5$ MHz in curve d; $V_c = 12.6$ MHz in curve e; $V_c = 13.9$ MHz in curve f.

$V_p = V_{e_i g_j}(\omega_p) = 0.89$ MHz ($j = i \pm 1$). Consider the real transition of $F_e = 2 \leftrightarrow F_g = 3$, in which five coupling fields V_c and ten probe fields V_p interact with the Zeeman sublevels, thus the total Rabi frequencies of coupling and probe fields (Z_c and Z_p) are five and ten times of V_c and V_p, respectively. Curve 'a' in figure 6(1) is the standard spectrum of EIT when we take $B = 0$ Gs; as experimentally measured in figure 3, when the magnetic field is present, the EIT window is divided into two windows due to the multi-coherence induced by the Zeeman multilevel states (curve 'b' with $B = 2.8$ Gs). We can see from curves c–f that, by increasing the magnetic field, the two transparency maxima of EIT windows are shifted its position from resonance to off resonance. Comparing figure 6(1) with figure 3, we find a qualitative agreement between theoretical and experimental results.

Then, when we fix the strength of magnetic field $B = 9.8$ Gs and the Rabi frequency of probe beam $V_p = 0.89$ MHz, it is seen that with the increase in the Rabi frequency of coupling light V_c, both the EIT windows become wider as shown in figure 7(1). Curves a, b, c, d, e and f are for 5.92 MHz, 8.17 MHz, 9.89 MHz, 11.5 MHz, 12.6 MHz and 13.9 MHz, the corresponding total Rabi frequencies are 29.6 MHz, 40.9 MHz, 49.5 MHz, 57.5 MHz, 63 MHz and 69.5 MHz. Obviously these effects are in agreement with the experimental data in figure 4.

The above derivation ignores Doppler broadening from the thermal motion of the atoms. The effects of Doppler broadening to the results can be included in the terms of laser detuning. In our experimental scheme, the drive and probe beams copropagate and their frequencies are very close, thus an atom moving towards the driven and probe beams with velocity v_z 'sees' their frequencies upshifted by an amount $k_{p,c}v_z$, and $k_{p,c}$ is the wave number for the coupling and probe laser, v_z dependent quantities thus obtained are then averaged over a given velocity distribution $f(v_z)$, which is the Gaussian distribution function of atomic velocities $f(v_z) = \frac{1}{v\sqrt{\pi}}e^{-v_z^2/v^2}$. Here we do not perform such average operation but merely give a qualitative analysis through replacing the detuning by $\Delta \Rightarrow \Delta + k_c v$ and $\delta \Rightarrow \delta + k_p v$ with $v \propto \sqrt{\langle v_z^2 \rangle}$ and $\langle v_z^2 \rangle = \int v_z^2 f(v_z)\,dv_z$, where $v = \sqrt{2k_B T/M}$ is the most probable speed of atoms at given temperature T, M is the atomic mass and k_B is the Boltzmann constant. In our numerical discussion, we set $k_{p,c}v = \Gamma$, with which the simulation curves (see figures 6(2)

and 7(2)) are approximately matched with the experiment results, in which the non-Lorentzian lineshapes of EIT windows are observed, thus we can conclude that the main reason for the unsymmetrical EIT resonances comes from the effect of the Doppler broadening.

4. Conclusion

The effects of widening and shifting the EIT windows are observed experimentally in a two-level system of Cs vapour cell with two orthogonal polarized laser beams. It is shown that the multi-coherence induced by Zeeman sublevels leads to the splitter of EIT windows, and furthermore, it also results in the shift of transparency maxima with increasing the Zeeman splitting. On the other hand, when we increase the Rabi frequency of the coupling field, the splitting two EIT windows become wider caused by the coherence between the Zeeman splitting and drive fields. These phenomena are well explained by optical Bloch equations for the transition $F_g = 3 \leftrightarrow F_e = 2$.

Acknowledgments

This research is supported by the National Natural Science Foundation of China (no. 60278010), Shanxi Natural Science Foundation (no. 20041039) and returned Scholar Foundation. The authors would like to thank Dr Ying Gu for helpful discussions.

References

[1] Boller K J, Imamolu A and Harris S E 1991 *Phys. Rev. Lett.* **66** 2593
[2] Akulshin A M, Barreiro S and Lezama A 1998 *Phys. Rev.* A **57** 2996
[3] Gray H R, Whitley R M and Stroud C R Jr 1978 *Opt. Lett.* **3** 218
[4] Harris S E 1989 *Phys. Rev. Lett.* **62** 1033
[5] Scully M O 1991 *Phys. Rev. Lett.* **67** 1855
[6] Phillips D F, Fleischhauer A, Mair A and Walsworth R L 2001 *Phys. Rev. Lett.* **86** 783
[7] Lee H, Fleischhauer M and Scully M O 1998 *Phys. Rev.* A **58** 2587
[8] Turchette Q A, Hood C J, Lange W, Mabuchi H and Kimble H J 1995 *Phys. Rev. Lett.* **75** 4710
[9] Harris S E and Yamamoto Y 1998 *Phys. Rev. Lett.* **81** 3611
[10] Boto A N, Kok P, Abrams D S, Braunstein S L, Williams C P and Dowling J P 2000 *Phys. Rev. Lett.* **85** 2733
[11] Akulshin A M, Barreiro S and Lezama A 1999 *Phys. Rev. Lett.* **83** 4277
[12] Lezama A, Barreiro S, Lipsich A and Akulshin A M 1999 *Phys. Rev.* A **61** 013801
[13] Lipsich A, Barreiro S, Akulshin A M and Lezama A 2000 *Phys. Rev.* A **61** 053803
[14] Goren C, Wilson-Gordon A D, Rosenbluh M and Friedmann H 2003 *Phys. Rev.* A **67** 033807
[15] Kim S K, Moon H S, Kim K and Kim J B 2003 *Phys. Rev.* A **68** 063813
[16] Gu Y, Sun Q and Gong Q 2003 *Phys. Rev.* A **67** 063809
[17] Gu Y, Sun Q and Gong Q 2004 *J. Phys. B: At. Mol. Opt. Phys.* **37** 1553
[18] Kim K, Moon H S, Lee C, Kim S K and Kim J B 2003 *Phys. Rev.* A **68** 013810
[19] Lezama A, Barreiro S and Akulshin A M 1999 *Phys. Rev.* A **59** 4732
[20] Fulton D J, Moseley R R, Shepherd S, Sinclair B D and Dunn M H 1995 *Opt. Commun.* **116** 231
[21] Boon J R, Mc Gloin E and Dunn M H 1999 *Phys. Rev.* A **59** 4675
[22] Steck D A 2003 http://steck.us/alkalidata
[23] Wilson-Gordon A D and Friedmann H 1983 *Opt. Lett.* **8** 617
[24] Boyd R W, Raymer M G, Narum P and Harter D J 1981 *Phys. Rev.* A **24** 411
[25] Kim M, Kim K, Moon H S, Park H D and Kim J B 2001 *J. Phys. B: At. Mol. Opt. Phys.* **34** 2951